analytical chemistry

Article

Cite This: *Anal. Chem.* 2018, 90, 12239−12245

pubs.acs.org/ac

"Axial" Magnetic Levitation Using Ring Magnets Enables Simple Density-Based Analysis, Separation, and Manipulation

Shencheng Ge[†] and George M. Whitesides*[,†,‡,§]

[†]Department of Chemistry and Chemical Biology, Harvard University, 12 Oxford Street, Cambridge, Massachusetts 02138, United States

[‡]Wyss Institute for Biologically Inspired Engineering, Harvard University, 60 Oxford Street, Cambridge, Massachusetts 02138, United States

[§]Kavli Institute for Bionano Science and Technology, Harvard University, 29 Oxford Street Cambridge, Massachusetts 02138, United States

Supporting Information

ABSTRACT: This work describes the development of magnetic levitation (MagLev) using ring magnets and a configuration (which we call "axial MagLev") to remove the physical barriers to physical sampling in the magnetic field present in "standard MagLev" and to simplify the procedures used to carry out density-based analyses, separations, and manipulations. The optimized, linear magnetic field generated between the two ring magnets (coaxially aligned and like-poles facing) enables the levitation of diamagnetic (and weakly paramagnetic, e.g., aluminum) materials in a paramagnetic suspending medium and makes density measurements more straightforward. This "axial" configuration enables (i) simple procedures to add samples and paramagnetic medium from an open end and to retrieve samples while levitating in the magnetic field (e.g., a subpopulation of a cluster of small particles); (ii) simple accesses and the abilities to view the samples 360° around the sample container and from the top and bottom; and (iii) convenient density measurements of small quantities (as small as a single submillimeter particle as demonstrated) of samples. The compact design, portability, affordability, and simplicity in use of the "axial MagLev" device will broaden the uses of magnetic methods in analyzing, separating, and manipulating different types of samples (solids, liquids, powders, pastes, gels, and also biological entities) in areas such as materials sciences, chemistry, and biochemistry.

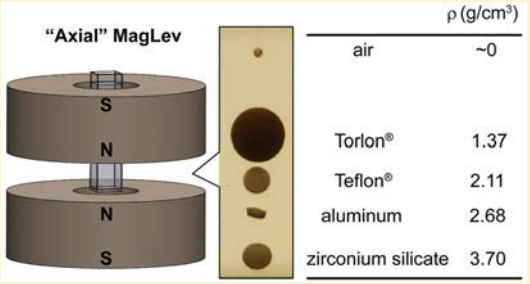

This work describes the development of "axial magnetic levitation (MagLev)" using ring magnets to remove the physical barriers to access the sample along the central axis of the magnetic field that can limit the commonly used "standard MagLev" device. Axial MagLev enables simple procedures with which to perform density-based (Magneto-Archimedean) analyses, separations, and manipulations. For example, density could be used to (i) separate and analyze different types of nonbiological and biological materials (e.g., glass, metals, crystal polymorphs, polymer particles, mammalian cells, yeasts, and bacteria);[1−3] (ii) monitor chemical processes that accompany changes in density, such as chemical reactions (e.g., chemical reactions on a solid support and polymerization) and binding events (e.g., ligands/enzymes, antibodies/antigens, and antibodies/cells);[4−9] (iii) perform contact-free orientation of objects and also self-assembly in 3D;[10,11] and (iv) quality-control injection-molded plastic parts.[12]

We and others[1,3,8,13−19] have been developing MagLev as a simple and useful technique to exploit density, a simple and universal physical property of all matter, for a range of applications in diverse areas, such as chemistry, biochemistry, and materials science. The "standard" configuration of MagLev as we and others commonly use it has a particular spatial arrangement of magnets in which the sample container (typically a standard square cuvette with a height of 45 mm) is sandwiched between two block NdFeB permanent magnets (Figure 1A).[3,13] This configuration makes it inconvenient (i) to add and remove the paramagnetic medium or the levitating samples (particularly those viscous or sticky samples), (ii) to observe the levitating sample from the top and bottom, (iii) to move the paramagnetic medium in the container along the central axis between the magnets, and (iv) to accommodate sample containers higher than the distance of separation between the magnets, such as tall vials and test tubes. During the preparation of this manuscript, Fu et al. reported a configuration of MagLev device using a single ring magnet and described a beautiful set of experiments that exploited the resulting axial, nonlinear magnetic field to carry out density-based manipulations and measurements.[20]

We positioned a pair of ring magnets with like-poles facing (analogous to the anti-Helmholtz configuration using electromagnets[21,22]) to engineer a linear, axially symmetric magnetic

Received: August 3, 2018
Accepted: September 13, 2018
Published: October 1, 2018

DOI: 10.1021/acs.analchem.8b03493
Anal. Chem. 2018, 90, 12239−12245

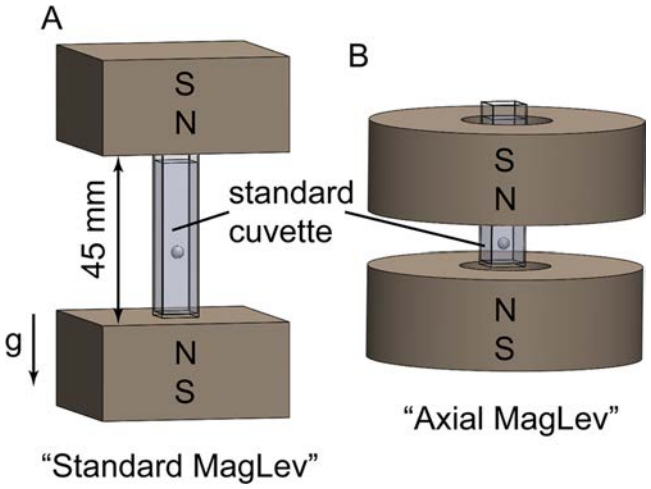

Figure 1. Overview of MagLev. (A) The "standard MagLev" device comprises two like-poles facing, block magnets (NdFeB permanent magnets, $W \times L \times H$: 50.8 mm × 50.8 mm × 25.4 mm) positioned coaxially with a distance of separation of 45.0 mm. A standard cuvette (45 mm in height) is a common container used to levitate diamagnetic samples (represented by a 3 mm sphere) in a paramagnetic medium (e.g., aqueous solutions of $MnCl_2$). The strength of the magnetic field is ∼0.38 T at the center of the top face of the bottom magnet (N52 grade). (B) The "axial MagLev" device uses two like-poles facing ring magnets (NdFeB permanent magnets, OD × ID × H: 76.2 mm × 25.4 mm × 25.4 mm) positioned coaxially with a distance of separation of 15.0 mm. The same cuvette containing the 3 mm sphere in (A) is included to show the size of the devices. The strength of the magnetic field is ∼0.33 T at the center of the top face of the bottom magnet (N45 grade).

field, and used it to levitate diamagnetic and weakly paramagnetic (e.g., aluminum) objects in a paramagnetic medium (e.g., aqueous solutions of $MnCl_2$ or $GdCl_3$) for density-based analyses, separations, and manipulations (Figure 1B). The use of a linear magnetic field between the ring magnets helps simplify the procedures with which to calibrate and carry out density measurements; the nonlinear portion of the magnetic field, particularly the field in the cavity of the ring magnet, could also be used to perform density-based separations and manipulations, as we (Figure S4) and others have demonstrated using permanent magnets or electromagnets.[20,23−26]

We optimized the size and aspect ratios of the magnets to yield a linear magnetic field. The maximum B_o along the central axis between the magnets is ∼0.33 T, and the linear magnetic field extends into the cavities of the ring magnets (approximately half of the distance of separation between the magnets). This geometry made it possible to perform density-based analyses and separations of diamagnetic and weakly paramagnetic samples and to exchange the paramagnetic medium surrounding the levitating objects (e.g., by moving the sample container relative to the magnets).

This configuration using two ring magnets makes a number of new procedures either accessible or more convenient than those described previously.[13,14] Because of the fact that both the top and bottom of the sample container are easily accessible in this "axial" configuration, it is, in particular, straightforward to recover samples and to exchange the paramagnetic medium surrounding the levitating objects without having to remove the sample container from the magnetic field.

EXPERIMENTAL DESIGN

Design of the Device. The general working principle of MagLev (Magneto-Archimedes levitation) is described elsewhere in detail.[13] Generally, a diamagnetic object levitates stably in a paramagnetic medium in an applied magnetic field when the buoyancy-corrected gravitational force and magnetic force acting on the object balance each other (Figure 2A).

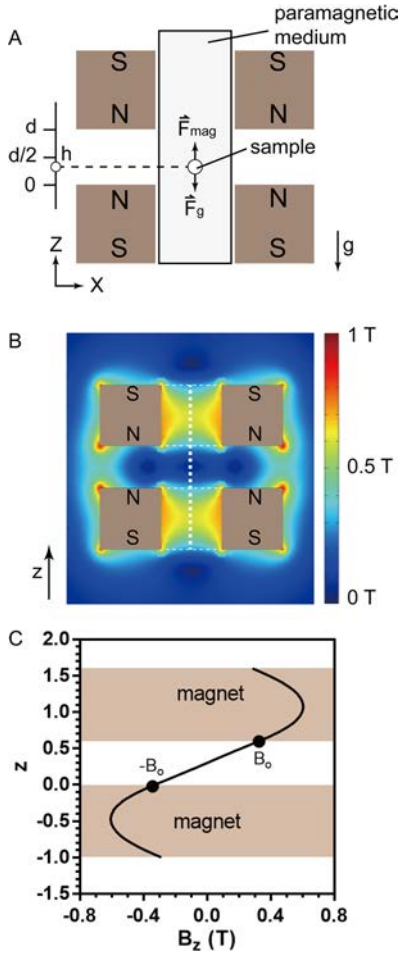

Figure 2. Design of the axial MagLev device using ring magnets: (A) Schematic shows a pair of indistinguishable magnets arranged coaxially with the like-poles facing (inner diameter/outer diameter/height/distance of separation = 1:3:1:0.6), and a diamagnetic object (sample) levitates in a paramagnetic medium. The z-axis of the setup is antialigned with the vector of gravity. (B) Spatial profile of the magnetic field on the vertical cross-section through the central axis (the central axis overlaps with the vertical dotted line). (C) Magnetic field strength, B_z, along the vertical dotted line in (B). B_o = ∼0.33 T for the configuration shown here using two N45-grade NdFeB permanent magnets. The z-axis is unitless for this plot.

Equation 1 describes the two types of physical forces the object experiences, and the sum of the forces is zero when the object reaches the equilibrium position.

$$\vec{F}_g + \vec{F}_{mag} = (\rho_s - \rho_m)V\vec{g} + \frac{(\chi_s - \chi_m)}{\mu_o}V(\vec{B}\cdot\vec{\nabla})\vec{B} = 0 \quad (1)$$

In eq 1, $\vec{F}_g$ is the buoyancy-corrected gravitational force, $\vec{F}_{mag}$ is the magnetic force, ρ_s (kg/m^3) is the density of the suspended object, ρ_m (kg/m^3) is the density of the para-

DOI: 10.1021/acs.analchem.8b03493
Anal. Chem. 2018, 90, 12239−12245

magnetic medium, $\vec{g}$ (-9.810 m/s^2) is the acceleration due to gravity, χ_m (unitless) is the magnetic susceptibility of the paramagnetic medium, χ_s (unitless) is the magnetic susceptibility of the suspended object, V (m^3) is the volume of the object, μ_o ($4\pi \times 10^{-7}$ N/A^{-2}) is the magnetic permeability of free space, $\vec{B}$ (T) is the magnetic field, and $\vec{\nabla}$ is the gradient operator.

When the magnetic field is linear and the z-component of the field dominates the contribution to the magnetic force, eq 1 can be simplified to give eqs 2 and 3. These equations form the theoretical basis of density-based separations, analyses, and manipulations (on which this work also rests).[13] B_o is the maximum strength of the linear magnetic field.

$$B_z = \frac{2B_o}{d}z - B_o \tag{2}$$

$$\rho_s = \alpha z + \beta \tag{3a}$$

$$\alpha = \frac{4(\chi_s - \chi_m)B_o^2}{\mu_o g d^2} \tag{3b}$$

$$\beta = \rho_m - \frac{2(\chi_s - \chi_m)B_o^2}{\mu_o g d} \tag{3c}$$

For the great majority of the diamagnetic objects (e.g., common organic solids, liquids, and gels) and weakly paramagnetic materials (e.g., aluminum) suspended in a concentrated paramagnetic medium (e.g., 1 M $MnCl_2$), we can safely assume that $\chi_m \gg \chi_s$ in eq 3 because χ_s is generally close to zero and, thus, is negligible. (A quantitative calculation is also available.[13])

We positioned two ring magnets (NdFeB permanent magnets) coaxially with the like-poles facing such that the gradient of the magnetic field between the magnets is linear, and then aligned its central axis with the vector of gravity. We simulated the magnetic field using Comsol (see SI for detailed information, including parameter space examined) to optimize the geometry of the ring magnets, including the inner diameter (id), the outer diameter (od), the height of the magnets (h), and the distance of separation between the magnets (d), to maximize the strength of the linear magnetic field between them (Figure 2). We took advantage of the "homothetic" property of the magnetic field generated by permanent magnet(s), that is, the spatial profile (that is its spatial distribution) of the magnet field remains unchanged, while the magnet(s) scale in physical size;[27] we thus focused first on optimizing the "aspect-ratio" of the magnets (i.e., id/od/h/d) to maximize the strength of the field (see Figure S1 and Table S1 for details). The results of these simulations suggest that the strength of the magnetic field between the magnets can be linear for B_o up to ~0.4 T (the highest achievable B_o is ~0.5 T for the parameter space examined). While we focused primarily on the linear gradient in the gap between the magnets, the entire range of the linear gradient, in fact, extends slightly into the cavities of the ring magnets and is approximately the size of the inner diameter of the ring magnet for the setup shown in Figure 1).

This study used two NdFeB ring magnets with the same shape (76 mm in outer diameter, 25 mm in inner diameter, and 25 mm in height) positioned apart by 15 mm. We made this choice because (i) this configuration generates a strong, linear field between the magnets (B_o = ~ 0.33T); (ii) it has a large working distance between the magnets (15 mm); (iii) the setup is compact and, thus, facilitates sample viewing (comparing to configurations using magnets with a larger ratio of od to id); (iv) the magnets are commercially available; and (v) the magnets are relatively inexpensive (~$50 per magnet). A 3D-printed plastic housing, metal rods, and screws were used to secure the magnets mechanically in space (Figure S2). (*Caution: magnets of this size generate strong forces when placed close to one another with the opposite-poles facing or close to other magnetizable objects (e.g., iron plate) and, thus, are a safety hazard and require careful handling. In particular, magnets should be handled at a sufficiently large distance from medical devices, such as pacemakers, that there are no risks.* Videos demonstrating the strong forces generated by NdFeB magnets are easily accessible from sources, such as https://www.youtube.com/watch?v=0t8yDnyOaQ8.)

A single ring magnet has two local minima in its field strength along its central axis (Figure S3), and this spatial profile of the field, albeit nonlinear along the central axis on either side, could also be used to levitate diamagnetic objects in a paramagnetic medium (Figure S4). Rings of different sizes and also in combination with one or more flux concentrators (e.g., soft iron plate) may also be used to "shape" the magnetic field and, thus, to levitate diamagnetic objects.

Choice of Paramagnetic Medium. We typically use an aqueous solution of a paramagnetic species (e.g., $MnCl_2$, $MnBr_2$, $CuSO_4$, $GdCl_3$, $DyCl_3$, $HoCl_3$, and Gd chelates such as gadolinium(III) diethylenetriaminepentaacetic acid) to suspend objects.[13] These paramagnetic species are inexpensive, transparent in the visible region of the spectrum (even at high concentrations), and commercially available. MagLev also works with hydrophobic paramagnetic medium and paramagnetic ionic liquids.[28,29]

Choice of Cross-Linked Polymeric Materials and Solvents to Measure the Swelling Ratios. We used "axial MagLev" as a simple analytical tool to measure the swelling ratios of cross-linked polymer materials, particularly those in irregular shapes and small quantities, in hydrophobic solvents by measuring the densities of both the dry and fully swollen samples using an aqueous $MnCl_2$ suspension medium.

The swelling ratio (the volumetric ratio) of a cross-linked polymer material characterizes its tendency to swell by absorption of solvents (that is, the absorption of a solvent into the cross-linked network of the material). This ratio reflects, in part, the cross-link density present in the polymeric material and the way in which the solvent interacts with polymeric chains; it is, therefore, a useful parameter in characterizing the cross-linked polymer in different fields,[30,31] such as solid-phase organic synthesis, development of superabsorbent materials, and use of polymeric materials for drug releasing applications.

A number of techniques to measure the swelling ratio of cross-linked polymeric materials include the use of graduated cylinders (to track the bulk volume, e.g., of a collection of particles), gravimetric techniques (to weigh the sample), optical microscopy (to measure the dimension of the sample), and specialized instrumentations.[32] These techniques, however, are generally tedious, require large quantity of samples (on the scale of grams), and have limited compatibility with different types of samples (e.g., irregularly shaped samples, powders, and delicate or gel-like materials).

We developed MagLev using the "axial" configuration as a simple and broadly compatible tool to measure the swelling

DOI: 10.1021/acs.analchem.8b03493
Anal. Chem. 2018, 90, 12239−12245

ratios of cross-linked polymeric materials in solvents. We chose cross-linked polydimethylsiloxane as a model material for this demonstration. In a previous study, we characterized the swelling behavior of PDMS in a variety of organic solvents (in the context of developing PDMS-based microfluidic devices).[33]

Because the MagLev technique (as we describe in this study) uses an aqueous $MnCl_2$ solution to levitate samples; the solvents used to swell PDMS samples should not dissolve in the aqueous solutions. Among the 39 solvents we characterized in the previous study,[33] we chose in this study the following three hydrophobic solvents for a demonstration: chloroform, chlorobenzene, and toluene. The use of water-miscible solvents will require the same compatibility of solubility of the sample (PDMS soaked with solvents) and the suspension medium (e.g., using hydrophobic Gd chelate dissolved in hydrophobic solvents) for which we did not demonstrate in this study.

RESULTS AND DISCUSSION

Calibration. We used hydrophobic organic liquids to calibrate the device: (i) They have known densities. Solubility of water in hydrophobic solvents we used in this study has a negligible influence on the density of the solvents. For instance, the solubility of water in chlorobenzene is 0.3 mol % at room temperature,[34] and the dissolved water only causes a change in its density less than 0.01%. We have previously evaluated the stability in levitation height of five hydrophobic solvents in an aqueous $MnCl_2$ solution, and found no apparent change in h over at least 30 min.[13] (ii) They can be used as small drops (1−2 mm in diameter), a characteristic that facilitates accurate localization of the centroid (in comparison to the ∼4 mm, often irregular-shaped standard glass beads that we have commonly used in previous studies[13]). (iii) They are commercially available. Figure 3 shows the levitation of five drops (added sequentially using a pipettor) of known densities in the same cuvette containing an aqueous solution of 0.5 M $MnCl_2$. The levitation heights of the drops did not change over 30 min we tested the stability of these levitating drops. We obtained, as expected, linear calibration curves ($R^2 > 0.999$).

Range of Densities That Can Be Measured. We levitated objects (Figure 4) using a concentrated aqueous solution of 3.0 M $DyCl_3$ that ranged from a bubble of air ($\rho \approx 0$ g/cm^3) to zirconium silicate ($\rho \approx 3.7$ g/cm^3). The combined use of a concentrated paramagnetic salt $DyCl_3$ with a high magnetic susceptibility ($DyCl_3$ 5.5×10^{-7} m^3/mol vs $MnCl_2$ 1.83×10^{-7} m^3/mol)[35] and a steep gradient in magnetic field strength (∼43 T/m in "axial MagLev" vs ∼17 T/m in "standard MagLev") led to a wider accessible range of densities (from ∼0 to ∼3.7 g/cm^3) than the range reported previously (∼0.8 to ∼3 g/cm^3) using aqueous media of $MnCl_2$ and the "standard MagLev" device.[13] "Tilted MagLev", a variant of "standard MagLev" in which the device is tilted with respect to the vector of gravity, and the sample partially rests on the wall of the sample container while levitating along the central axis of the device, can measure the entire range of densities observed in matter at ambient conditions (from ∼0 to ∼23 g/cm^3);[14] this study, however, demonstrated a range that was expanded beyond that of previous studies using the "standard MagLev" device, but was experimentally much more convenient, and avoided some of the potential problems of "tilted MagLev" (e.g., the samples rest on the walls of the sample container).

Simple Procedures To Add and Retrieve Samples. The "axial" configuration conveniently enables simple experimental protocols to add and retrieve samples from the container. We demonstrated the simple procedures by levitating "sticky" samples (a drop of viscous liquid polydimethylsiloxane prepolymer and a plug of Vaseline gel, Figure 5), a type of sample that is inconveniently measured using the "standard MagLev" and "tilted MagLev" devices (as the samples tend to stick to the walls of the container, and also to the liquid−air interface). The "axial" configuration also readily enables simple procedures to retrieve a targeted fraction of a sample (e.g., from a collection of particles).

We placed a test tube filled with a paramagnetic medium in the MagLev device and dropped in the "sticky" samples from its top; the sample entered the medium by gravity and levitated in it (nearly instantaneously for mm-sized samples, Figure 5).

Retrieving a sample from the container placed in the MagLev device is straightforward due to its axial configuration. As a demonstration, we used a simple procedure and the device to improve the precision (that is the spread of densities) of the density standards (polyethylene particles, ∼200 μm in diameter and 1.13 g/cm^3 in nominal density, provided by the vendor).[36] We inserted a glass Pasteur pipet with its tip bent ∼90° using flame from the top to the sample container (a test

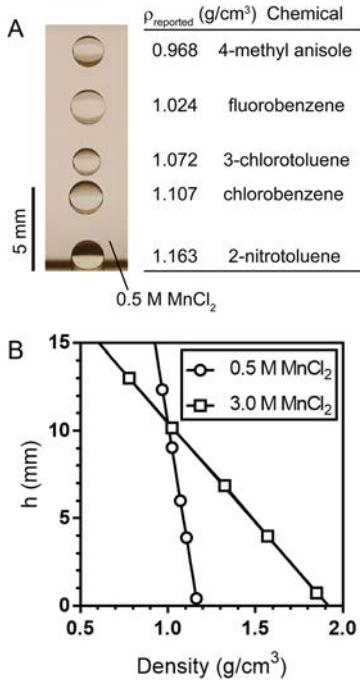

Figure 3. Calibration of the device using water-insoluble organic liquids. (A) A string of drops (∼3 μL) of organic liquids were sequentially added and levitated in an aqueous solution of 0.5 M $MnCl_2$ in a square cuvette. (B) Calibration curves using aqueous $MnCl_2$ solutions. We placed a ruler with millimeter marks next to the cuvette (we read to ±0.1 mm), and used a digital camera to take a photo of the drops. Levitation height h is the distance between the centroid of the drop and the upper surface of the bottom magnet (see Figure 2A for an illustration of h). Organic liquids used to calibrate the solution of 3.0 M $MnCl_2$ are cyclohexane (ρ = 0.779 g/cm^3), fluorobenzene (ρ = 1.024 g/cm^3), dichloromethane (ρ = 1.325 g/cm^3), 1,1,2-trichlorotrifluoroethane (ρ = 1.57 g/cm^3), and FC40 (ρ = 1.85 g/cm^3). The equations for the linear fits are $h = -61.5\rho + 71.9$ (R^2 = 0.9997) for 0.5 M $MnCl_2$, and $h = -11.4\rho + 21.9$ (R^2 = 0.9999) for 3.0 M $MnCl_2$. All densities are reported values by sigma.com. The data are plotted as mean ± standard deviation (N = 7 for all measurements). The error bars are much smaller than the size of the symbols and, thus, are invisible on the plot.

DOI: 10.1021/acs.analchem.8b03493
Anal. Chem. 2018, 90, 12239−12245

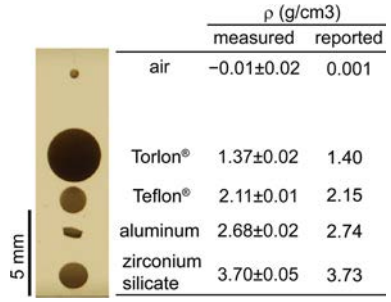

Figure 4. Expanded range of densities using "axial MagLev" and an aqueous solution of 3.0 M $DyCl_3$ containing 0.01 v% Tween-20. All samples are spheres except that the aluminum sample is irregular in shape (cut from a sheet of foil, 250 μm thickness). We used a typical square cuvette (1 cm path length) to levitate the samples and the following solvents to calibrate the device: cyclohexane (ρ = 0.779 g/cm^3), dichloromethane (ρ = 1.325 g/cm^3), 1,2-dibromoethane (ρ = 2.18 g/cm^3), and tribromomethane (ρ = 2.89 g/cm^3). Linear fit gave $h = -3.43\rho + 12.9$ (R^2 = 0.9999). The reported densities were obtained from sources listed in the SI (including the commercial vendors from which we purchased the materials, mcmaster.com and sigmaaldrich.com). N = 7 measurements for all samples.

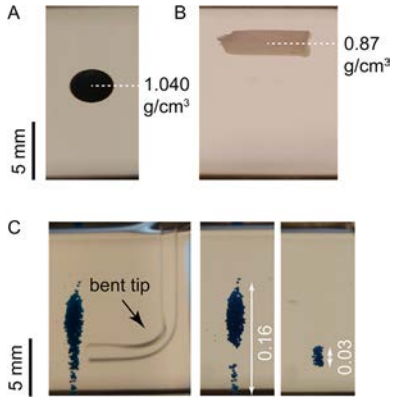

Figure 5. Simple procedures to add or retrieve samples. (A) A drop of liquid polydimethylsiloxane prepolymer (doped with black graphite powder for better visualization) levitated in an aqueous solution of 0.5 M $MnCl_2$. The drop appeared elliptical due to the visual distortion by the curved wall of the cylindrical test tube. (B) A plug of Vaseline gel extruded from a syringe levitated in an aqueous solution of 3.0 M $MnCl_2$ with 0.1% (v/v%) Tween-20. (C) Retrieval of a subpopulation of density standard beads. The beads that were retrieved levitated at the same height from which they were removed originally (third panel). The suspension solution contained 0.5 M $MnCl_2$, 1.4 M NaCl (a diamagnetic cosolute used to match the densities of the particles and the solution), and 0.1% Tween-20. White arrows indicate the spread in density of the particles (unit: g/cm^3).

tube with a diameter of ~25 mm) and removed a subpopulation of particles that levitated in an aqueous $MnCl_2$ solution. The rest of the sample remained levitated and undisturbed; the removed fraction levitated, expectedly, at the same height in the same media when placed back to the device (Figure 5C), but has a ~5× narrower distribution in density (thus, improved precision). MagLev, thus, provides a simple and straightforward method to prepare high-quality density standards.

Simple Analytical Tool to Measure the Swelling Ratios of Cross-Linked Polymers in Solvents. We chose PDMS as a model cross-linked polymer to demonstrate the use of "axial MagLev" in characterizing the swelling behavior of cross-linked polymers in solvents. We immersed a small piece of PDMS (1.5 mm in diameter and ~1 mm in thickness, prepared by a 1.5 mm biopsy punch) in solvent for 24 h. The sample was blotted dry and added to the MagLev device for density measurement using an aqueous 1.5 M $MnCl_2$ solution with 0.1 v% cetyltrimethylammonium bromide (a surfactant to help remove air bubbles). MagLev measures the density of the sample directly, irrespective of its volume (or shape). We converted the measured densities to the volumetric swelling ratio (Table 1) using eq 1 (see SI for derivation).

$$f = \frac{V_{sp}}{V_p} = \frac{\rho_p - \rho_{sol}}{\rho_{sp} - \rho_{sol}} \quad (4)$$

Table 1. Swelling Ratios of PDMS Samples in Solvents

	volumetric swelling ratio f		
	MagLev[a]	imaging[b]	literature[c]
$CHCl_3$	2.1	1.9	2.7
chlorobenzene	2.2	2.1	1.8
toluene	2.2	2.2	2.2

[a]The reported value is the average of three measurements. [b]The volumetric swelling ratio was calculated using the following equation $f = (D/D_0)^3$, where D is the diameter of the swollen PDMS disc and D_0 is the diameter of the dry PDMS disc. We assumed isotropic swelling of PDMS samples in the solvents. N = 3. [c]We have previously measured[33] the swelling ratios of small pieces of PDMS, and obtained the following ratios of the length of a swollen PDMS sample to a dry sample: chloroform 1.39, chlorobenzene 1.22, toluene 1.31. These values were converted to volumetric swelling ratios.

In eq 4, V_{sp} is the volume of the swollen sample, V_p is the volume of the dry sample, ρ_p is the density of the sample, ρ_{sp} is the volume of the swollen sample, and ρ_{sol} is the density of the solvent.

We also measured the diameters of the dry and swollen samples from the same images we measured the levitation heights and estimated the swelling ratio. The agreement of the results (within 10% deviation) validates the performance of the MagLev technique. The difference from the literature values may have originated from different sample preparations. (We did not investigate this difference further.) This demonstration also highlights the simplicity and compatibility of the MagLev technique in measuring small quantities of samples without requiring more sophisticated tools (e.g., microscopes).

CONCLUSION

This study describes the development of "axial" MagLev that exploits the axially symmetric magnetic field generated by two like-poles facing ring magnets to carry out density-based analyses, separations, and manipulations. This configuration of MagLev removes the physical barriers along the central axis of the commonly used MagLev devices in which sample containers (e.g., square cuvette and capillary tubes) are physically sandwiched between two block magnets. It has four useful characteristics: (i) it provides easy accesses to the levitating sample and the paramagnetic medium, and makes it straightforward to add/or remove the sample or the suspending medium; (ii) it maintains full clearance (360°) around the sample container to view the levitating samples, and also provides easy accesses to view the samples from both the top and the bottom; (iii) it does not impose a limitation on

DOI: 10.1021/acs.analchem.8b03493
Anal. Chem. 2018, 90, 12239−12245

the height of the sample container and is broadly compatible with different types of containers (cuvettes, vials, test tubes, graduated cylinders, etc.) so long as they fit within the inner diameter of the ring magnets; and (iv) it concentrates small and/or dilute particles along a common vertical axis and aids in their visualization and manipulations.

The major advantages of the two-ring system over the single-ring system[20] are the following: (i) The use of an engineered linear magnetic field in the two-ring system, rather than the nonlinear magnetic fields generated by a single ring magnet, enables simple, straightforward procedures to carry out density-based measurements, including performing calibrations and adjusting the sensitivity and dynamic range of the system. (ii) The two-magnet system enables the design of a linear magnetic field gradient between the magnets. (iii) The particles tend to align along the centerline connecting the centers of the two ring magnets. (iv) The operational simplicity in carrying out density-based separations makes possible an expanded range of densities. In the single-ring system, the accessible range of densities is physically divided into two segments: one in which samples less-dense than the liquid medium levitate ($\rho_s < \rho_m$) below the ring magnet and the one in which more-dense samples levitate ($\rho_s > \rho_m$) above it.[20] This particular spatial arrangement of ranges in density makes the separation of samples into subpopulations inconvenient because separations of samples occur independently within either segments, that is, for example, the materials (e.g., a suspension of microparticles) more dense than the suspending medium will either levitate in the solution for the segment above the magnet or sink to the bottom of the sample container for the segment below the magnet; the materials having the same density will, therefore, appear as two clusters in the sample container. Separations are more complex when the samples are heterogeneous in density. The two-ring system, however, combines these two segments as a single range and makes it possible to carry out straightforward separations and fractionation (for samples homogeneous or heterogeneous in density).

The major shortcoming of this axial design, in comparison to the "standard MagLev", is its relatively short working distance (~15 mm vs 45 mm in the "standard MagLev" device). This distance is determined by the physical size of the ring magnets (which are in turn limited by the commercial availability); larger ring magnets could, in principle, extend the working distance. While we, in this study, focused on the use of a linear magnetic field between the ring magnets to carry out density-based measurements, separations, and manipulations, nonlinear magnetic fields between the magnets could also be used. In this case, the working distance between the two magnets can be extended at least to ~38 mm, while the monotonically changing gradient in magnetic field (and, thus, density) is still maintained for simple operations (Figure S1E).

Density is a universal property of all matter, and a simple, inexpensive, and useful MagLev device such as the one described in this study will broaden the use of density in chemistry, biochemistry, and materials science. In particular, the compact design, portability, affordability, and simplicity in the use of the "axial MagLev" device will enable its potential uses in characterization of materials (e.g., the swelling behavior of cross-linked polymeric materials in solvents as described in the study) and separations of samples (particularly small quantities, such as crystals) and in manipulating samples (both hard and soft, sticky objects, such as gels) without physical contact.

■ ASSOCIATED CONTENT

Supporting Information

The Supporting Information is available free of charge on the ACS Publications website at DOI: 10.1021/acs.analchem.8b03493.

Materials and the associated densities; Correlation of swelling ratio and densities; Figure S1. Selection of the geometry and the distance of separation between the ring magnets using Comsol simulation; Table S1. Optimization of the magnetic field using Comsol simulations; Figure S2. Assembly of the device; Figure S3. Magnetic levitation using a single ring magnet; Figure S4. Separation in a single-ring system (PDF).

■ AUTHOR INFORMATION

Corresponding Author

*E-mail: gwhitesides@gmwgroup.harvard.edu.

ORCID

George M. Whitesides: 0000-0001-9451-2442

Notes

The authors declare no competing financial interest.

■ ACKNOWLEDGMENTS

This work was funded by the U.S. Department of Energy, Office of Basic Energy Sciences, Division of Materials Sciences and Engineering under Award Number ER45852. Specifically, the DOE grant provided the salary for S.G. and supported the design of the MagLev device and its use to perform density measurements.

■ REFERENCES

(1) Winkleman, A.; Perez-Castillejos, R.; Gudiksen, K. L.; Phillips, S. T.; Prentiss, M.; Whitesides, G. M. *Anal. Chem.* **2007**, *79* (17), 6542−6550.

(2) Atkinson, M. B.; Bwambok, D. K.; Chen, J.; Chopade, P. D.; Thuo, M. M.; Mace, C. R.; Mirica, K. A.; Kumar, A. A.; Myerson, A. S.; Whitesides, G. M. *Angew. Chem., Int. Ed.* **2013**, *52* (39), 10208−11.

(3) Durmus, N. G.; Tekin, H. C.; Guven, S.; Sridhar, K.; Arslan Yildiz, A.; Calibasi, G.; Ghiran, I.; Davis, R. W.; Steinmetz, L. M.; Demirci, U. *Proc. Natl. Acad. Sci. U. S. A.* **2015**, *112* (28), 3661−8.

(4) Ge, S.; Semenov, S. N.; Nagarkar, A. A.; Milette, J.; Christodouleas, D. C.; Yuan, L.; Whitesides, G. M. *J. Am. Chem. Soc.* **2017**, *139* (51), 18688−18697.

(5) Shapiro, N. D.; Mirica, K. A.; Soh, S.; Phillips, S. T.; Taran, O.; Mace, C. R.; Shevkoplyas, S. S.; Whitesides, G. M. *J. Am. Chem. Soc.* **2012**, *134* (12), 5637−46.

(6) Shapiro, N. D.; Soh, S.; Mirica, K. A.; Whitesides, G. M. *Anal. Chem.* **2012**, *84* (14), 6166−72.

(7) Subramaniam, A. B.; Gonidec, M.; Shapiro, N. D.; Kresse, K. M.; Whitesides, G. M. *Lab Chip* **2015**, *15* (4), 1009−1022.

(8) Andersen, M. S.; Howard, E.; Lu, S. L.; Richard, M.; Gregory, M.; Ogembo, G.; Mazor, O.; Gorelik, P.; Shapiro, N. I.; Sharda, A. V.; Ghiran, I. *Lab Chip* **2017**, *17* (20), 3462−3473.

(9) Castro, B.; Sala de Medeiros, M.; Sadri, B.; Martinez, R. V. *Analyst* **2018**, *143*, 4379.

(10) Subramaniam, A. B.; Yang, D.; Yu, H. D.; Nemiroski, A.; Tricard, S.; Ellerbee, A. K.; Soh, S.; Whitesides, G. M. *Proc. Natl. Acad. Sci. U. S. A.* **2014**, *111* (36), 12980−12985.

(11) Mirica, K. A.; Ilievski, F.; Ellerbee, A. K.; Shevkoplyas, S. S.; Whitesides, G. M. *Adv. Mater.* **2011**, *23* (36), 4134−40.

DOI: 10.1021/acs.analchem.8b03493
Anal. Chem. 2018, 90, 12239−12245

(12) Hennek, J. W.; Nemiroski, A.; Subramaniam, A. B.; Bwambok, D. K.; Yang, D.; Harburg, D. V.; Tricard, S.; Ellerbee, A. K.; Whitesides, G. M. *Adv. Mater.* **2015**, *27* (9), 1587−1592.
(13) Mirica, K. A.; Shevkoplyas, S. S.; Phillips, S. T.; Gupta, M.; Whitesides, G. M. *J. Am. Chem. Soc.* **2009**, *131* (29), 10049−58.
(14) Nemiroski, A.; Soh, S.; Kwok, S. W.; Yu, H. D.; Whitesides, G. M. *J. Am. Chem. Soc.* **2016**, *138* (4), 1252−7.
(15) Nemiroski, A.; Kumar, A. A.; Soh, S.; Harburg, D. V.; Yu, H. D.; Whitesides, G. M. *Anal. Chem.* **2016**, *88* (5), 2666−74.
(16) Tasoglu, S.; Khoory, J. A.; Tekin, H. C.; Thomas, C.; Karnoub, A. E.; Ghiran, I. C.; Demirci, U. *Adv. Mater.* **2015**, *27* (26), 3901−8.
(17) Xia, N.; Zhao, P.; Xie, J.; Zhang, C. Q.; Fu, J. Z. *Polym. Test.* **2017**, *63*, 455−461.
(18) Xia, N.; Zhao, P.; Xie, J.; Zhang, C. Q.; Fu, J. Z. *Polym. Test.* **2018**, *66*, 32−40.
(19) Ge, S.; Wang, Y.; Deshler, N. J.; Preston, D. J.; Whitesides, G. M. *J. Am. Chem. Soc.* **2018**, *140* (24), 7510−7518.
(20) Zhang, C.; Zhao, P.; Gu, F.; Xie, J.; Xia, N.; He, Y.; Fu, J. *Anal. Chem.* **2018**, *90*, 9226.
(21) Enomoto, Y.; Kuroda, N.; Michishio, K.; Kim, C. H.; Higaki, H.; Nagata, Y.; Kanai, Y.; Torii, H. A.; Corradini, M.; Leali, M.; Lodi-Rizzini, E.; Mascagna, V.; Venturelli, L.; Zurlo, N.; Fujii, K.; Ohtsuka, M.; Tanaka, K.; Imao, H.; Nagashima, Y.; Matsuda, Y.; Juhasz, B.; Mohri, A.; Yamazaki, Y. *Phys. Rev. Lett.* **2010**, *105* (24), 243401.
(22) Migdall, A. L.; Prodan, J. V.; Phillips, W. D.; Bergeman, T. H.; Metcalf, H. J. *Phys. Rev. Lett.* **1985**, *54* (24), 2596−2599.
(23) Grzybowski, B. A. Static and Dynamic Self-Organization. *Ph.D. Thesis*, Harvard University, Cambridge, MA, August, 2000.
(24) Timonen, J. V.; Demirors, A. F.; Grzybowski, B. A. *Adv. Mater.* **2016**, *28* (18), 3453−9.
(25) Timonen, J. V. I.; Grzybowski, B. A. *Adv. Mater.* **2017**, *29* (18), 1603516.
(26) Parfenov, V. A.; Koudan, E. V.; Bulanova, E. A.; Karalkin, P. A.; Pereira, F. D. A. S.; Norkin, N. E.; Knyazeva, A. D.; Gryadunova, A. A.; Petrov, O. F.; Vasiliev, M. M.; Myasnikov, M. I.; Chernikov, V. P.; Kasyanov, V. A.; Marchenkov, A. Y.; Brakke, K.; Khesuani, Y. D.; Demirci, U.; Mironov, V. A. *Biofabrication* **2018**, *10* (3), 034104.
(27) Cugat, O.; Delamare, J.; Reyne, G. *IEEE Trans. Magn.* **2003**, *39* (6), 3607−3612.
(28) Mirica, K. A.; Phillips, S. T.; Mace, C. R.; Whitesides, G. M. *J. Agric. Food Chem.* **2010**, *58* (11), 6565−9.
(29) Bwambok, D. K.; Thuo, M. M.; Atkinson, M. B.; Mirica, K. A.; Shapiro, N. D.; Whitesides, G. M. *Anal. Chem.* **2013**, *85* (17), 8442−7.
(30) Santini, R.; Griffith, M. C.; Qi, M. *Tetrahedron Lett.* **1998**, *39* (49), 8951−8954.
(31) Ono, T.; Sugimoto, T.; Shinkai, S.; Sada, K. *Nat. Mater.* **2007**, *6*, 429.
(32) Maleki, A.; Beheshti, N.; Zhu, K. Z.; Kjoniksen, A. L.; Nystrom, B. *Polym. Bull.* **2007**, *58* (2), 435−445.
(33) Lee, J. N.; Park, C.; Whitesides, G. M. *Anal. Chem.* **2003**, *75* (23), 6544−54.
(34) Kirchnerová, J.; Cave, G. C. B. *Can. J. Chem.* **1976**, *54* (24), 3909−3916.
(35) Pulko, B.; Yang, X.; Lei, Z.; Odenbach, S.; Eckert, K. *Appl. Phys. Lett.* **2014**, *105* (23), 232407.
(36) Bloxham, W. H.; Hennek, J. W.; Kumar, A. A.; Whitesides, G. M. *Anal. Chem.* **2015**, *87* (14), 7485−7491.

DOI: 10.1021/acs.analchem.8b03493
Anal. Chem. 2018, 90, 12239−12245